THE PLASMA INSTRUMENTATION FOR THE GALILEO MISSION

L. A. FRANK, K. L. ACKERSON, J. A. LEE, M. R. ENGLISH, and G. L. PICKETT

Department of Physics and Astronomy, The University of Iowa, Iowa City, IA 52242, U.S.A.

Abstract. The plasma instrumentation (PLS) for the Galileo Mission comprises a nested set of four spherical-plate electrostatic analyzers and three miniature, magnetic mass spectrometers. The three-dimensional velocity distributions of positive ions and electrons, separately, are determined for the energy-per-unit charge (E/Q) range of 0.9 V to 52 kV. A large fraction of the 4π-steradian solid angle for charged particle velocity vectors is sampled by means of the fan-shaped field-of-view of 160°, multiple sensors, and the rotation of the spacecraft spinning section. The fields-of-view of the three mass spectrometers are respectively directed perpendicular and nearly parallel and anti-parallel to the spin axis of the spacecraft. These mass spectrometers are used to identify the composition of the positive ion plasmas, e.g., H^+, O^+, Na^+, and S^+, in the Jovian magnetosphere. The energy range of these three mass spectrometers is dependent upon the species. The maximum temporal resolutions of the instrument for determining the energy (E/Q) spectra of charged particles and mass (M/Q) composition of positive ion plasmas are 0.5 s. Three-dimensional velocity distributions of electrons and positive ions require a minimum sampling time of 20 s, which is slightly longer than the spacecraft rotation period. The two instrument microprocessors provide the capability of inflight implementation of operational modes by ground-command that are tailored for specific plasma regimes, e.g., magnetosheath, plasma sheet, cold and hot tori, and satellite wakes, and that can be improved upon as acquired knowledge increases during the tour of the Jovian magnetosphere. Because the instrument is specifically designed for measurements in the environs of Jupiter with the advantages of previous surveys with the Voyager spacecraft, first determinations of many plasma phenomena can be expected. These observational objectives include field-aligned currents, three-dimensional ion bulk flows, pickup ions from the Galilean satellites, the spatial distribution of plasmas throughout most of the magnetosphere and including the magnetotail, and ion and electron flows to and from the Jovian ionosphere.

1. Introduction

Although the first direct detection of the presence of plasmas in the vicinity of Io's orbit was reported by Frank *et al.* (1976) with measurements from the plasma analyzer on Pioneer 10, the first definitive measurements of Jovian magnetospheric plasmas were acquired during the Voyager flybys. The Voyager plasma observations were used to define the required capabilities for the Galileo plasma instrumentation. Briefly we summarize here the plasma domains of the Jovian magnetosphere. This information is largely taken from the review by Belcher (1983). For more recent work the reader is referred to further analysis of the torus ions (Bagenal, 1985; Bagenal *et al.*, 1985), the torus electrons (Sittler and Strobel, 1987), and the middle magnetosphere (Sands and McNutt, 1988). Measurements of medium-energy charged particles, $E \gtrsim 30$ keV, are summarized by Krimigis and Roelof (1983).

The heart of the Jovian magnetosphere is the great torus of plasmas that encompasses the orbit of Io. This torus is fed by the ionization of neutral gases from Io's atmosphere and may respond to the sporadic injection of gases from this moon's volcanic activity.

Space Science Reviews **60:** 283–307, 1992.

The composition of the ion plasmas in this torus is rich in heavy ions, e.g., S^+, O^+, S^{2+}, O^{2+}, and Na^+. The plasma torus is divided into two regimes, a cold torus inside Io's orbit and a hot torus at greater Jovicentric distances. The maximum ion densities, ~ 3000 cm^{-3}, are located near Io's orbit. The ion temperature decreases severely from ~ 40 eV at 6 R_J (Jovian radii) to ~ 1 eV at 5 R_J. This temperature decrease is due to radiative cooling. Ion temperatures in the hot torus at radial distances ~ 6 to 8 R_J are in the range of 40 to 100 eV. The electron temperatures can be described in terms of a two-temperature Maxwellian distribution, i.e., a cold and hot distribution. At the inner edge of the torus the electron temperatures decrease to ~ 0.5 eV with decreasing radial distances whereas the cold electron temperatures beyond ~ 6 R_J are typically ~ 10 to 100 eV. Characteristic temperatures of the hot electron velocity distributions are ~ 1 keV and the number densities are less than those for the cold electrons. The torus plasmas corotate with the planet. The corresponding corotational energy of an S^+ ion is 960 eV at equatorial radial distance 6 R_J. The deflection of plasma bulk flow near the Io flux tube is consistent with that expected for incompressible flow around a cylinder and is evidence for an Alfvén wave associated with the plasma flow past Io. The estimated current in the Io flux tube is $\sim 3 \times 10^6$ A, presumably carried in large part by electrons.

At distances beyond the plasma torus, $\gtrsim 10$ R_J, a plasma sheet extends to the dayside magnetopause. At 15 R_J the typical thickness of the plasma sheet is ~ 2 R_J. These plasmas are observed to corotate more-or-less rigidly with Jupiter's rotational motion to radial distances of about 20 R_J. At distances of 20 to 40 R_J this azimuthal bulk speed of the plasma is less than that expected from rigid corotation by factors of 2 or more. Beyond 40 R_J the plasmas are again observed to rigidly corotate at frequent times as inferred from measurements with the medium-energy charged particle detector. The corotational energy of an S^+ ion at 40 R_J is 43 keV. Whereas the density of the hot electrons is only $\sim 1\%$ of the total density at 8 R_J, the hot electron density is similar to that for the cold electrons at 40 R_J. Ion temperatures are also higher in the plasma sheet relative to those in the torus, ~ 20 to 40 keV at radial distances 30 to 100 R_J. Plasma densities in the plasma sheet are ~ 1 to 10 cm^{-3} at 10 to 20 R_J and vary from $\sim 10^{-3}$ to 1 cm^{-3} at larger radial distances. Above and below the plasma sheet the densities can be as low as 10^{-5} to 10^{-4} cm^{-3}.

Beyond radial distances of 130 R_J in the dawn side of the Jovian magnetosphere the ion bulk flows become generally anti-sunward with a strong component along directions that are radially outward from the planet. This region was detected with the medium-energy charged particle detector and is called the magnetospheric wind.

2. Advantages of the Galileo Plasma Measurements

The Galileo Mission advantages for plasma investigations in the Jovian magnetosphere are (1) the spinning section of the spacecraft, (2) an instrument microprocessor to restructure the instrument operation by ground command, and (3) a series of orbits that allow close flybys of the Galilean satellites, a survey of the Jovian magnetotail, and a

substantial local-time survey of the magnetosphere. The spinning section of the spacecraft provides the important capability for a suitably designed instrument to view the entire 4π-steradian solid angle for particle velocity vectors at the spacecraft position. The instrument microprocessor can be used to tailor the operation of the plasma instrument for the most effective measurements in each of the diverse plasma regimes of the magnetosphere and its environs, e.g., magnetosheath, plasma sheet, satellite wake or flux tube, or magnetospheric wind. Targeted encounters with the satellites and a tour of the magnetosphere and magnetotail offer exceptional opportunities for studies of most of the important plasma regions and their temporal responses to variations of Iogenic and solar wind plasmas, and the interactions of magnetospheric plasmas with the satellites.

The Galileo plasma instrumentation (PLS) is substantially more capable for measurements of the Jovian plasmas than those of the Pioneer and Voyager spacecraft because it is specifically designed for this purpose. The basic advantages are in the performance areas of (1) extended energy range, (2) coverage of the angular distributions of plasmas, (3) angular resolution, (4) temporal resolution, and (5) ion composition.

The energy-per-unit charge ranges of the Pioneer and Voyager plasma instruments are 100 to 4800 V and 10 to 5920 V, respectively. The corresponding range of the Galileo plasma analyzer is 0.9 to 52 000 V. This extended energy range spans the important energy gap between 5920 and 30 000 V in the combined performances for the Voyager plasma instrument and medium-energy particle detectors. The 4π-steradian solid angle for particle velocity vectors at the spacecraft position is sampled adequately to provide determinations of the three-dimensional velocity distributions for positive ions and electrons. Thus such important plasma parameters as field-aligned currents, cross-field currents, plasma bulk flow velocities, heat fluxes, and free energy are to be determined for the first time with the Galileo instrument. The angular resolution is sufficient to provide definitive measurements of the above plasma parameters. Temporal resolutions for obtaining electron and positive ion spectra are about 200 s for the Pioneer analyzer (ions only) and about 100 s for the Voyager Faraday cups. The corresponding temporal resolution for the Galileo plasma analyzer is about 0.5 s; complete three-dimensional velocity distributions for positive ions and electrons can be telemetered once each 20 s. These improved temporal resolutions are particularly important during the brief encounters with the satellites and the traversals of plasma boundaries such as those of the plasma sheet and current sheet in the middle and outer magnetospheres.

Three miniature mass spectrometers which are positioned at the exit apertures of the electrostatic analyzers in the Galileo instrument provide determinations of the positive ion composition. The Voyager determinations of ion composition from E/Q spectra are model-dependent and are possible when the Mach number of the corotational flow is greater than 5 or 6. This method is acceptable generally near the Io orbit but as the Jovian radial distance increases, ion thermal speeds rapidly increase and prevent decisive identification of ion species. The Galileo mass spectrometers provide a direct determination of ion composition, specifically the mass-per-unit charge.

In addition to the above performance features, the Galileo plasma analyzer can be

operated flexibly via electronic reconfiguration by ground command. The operational configuration of energy-per-unit charge (E/Q) passbands, mass-per-unit charge (M/Q) channels, sensors, and angular sectors can be tailored for a specific plasma region. The temporal resolution for a given measurement can also be selected. The Galileo plasma analyzer is equipped with sufficient onboard hardware and software to implement automated beam capture modes for ion velocity distributions and for determination of ion composition.

3. Several Anticipated Scientific Results

The capabilities of the Galileo plasma instrumentation are demonstrated here by application to several plasma regimes in the Jovian magnetosphere.

As the Galileo spacecraft crosses the plasma sheet in the middle and outer magnetospheres the magnitudes of field-aligned and cross-field currents are determined. Their values and location are correlated with the position of the current sheet as found with the magnetometer. The motions of the plasma sheet are directly determined from the three-dimensional bulk flow vector and the azimuthal component is separated from the radial outflow or inflow. Angular distributions and ion compositions are examined in order to discern the contributions of electrons and ions from the ionosphere, the solar wind via the magnetosheath, and Io in the inner magnetosphere. Thus the formation and dynamics of the plasma sheet can be understood. The mechanism for the unusual heating of plasma with increasing radial distance is expected to be identified.

The encounters with the Galilean satellites offer exciting opportunities for observing plasma phenomena. Examination of the ion velocity distributions in the wakes of these satellites is used to determine the mechanism for ion loss from these bodies. The effectiveness of ion pickup by the magnetospheric plasma flow is derived from the signatures in the velocity distributions of these ions. The mass spectrometers are used to identify the major ions produced in the vicinity of the satellite. For Io these ions include O^+, S^+, and SO_2^+, and for icy satellites perhaps H^+, C^+, and H_2O^+ can be found. Such measurements give the rate of mass loss from each satellite. Perturbations of the plasma flow can be identified in terms of the conductivity of the satellite. During the closest satellite encounters it is possible that a magnetopause or ionopause is detected, thus providing further information concerning the magnetic and atmospheric properties of that body. If the flyby of the satellite is polar, detection of strong field-aligned currents to and away from the Jovian ionosphere might be expected. Field-aligned acceleration of ions and electrons by electrostatic double layers or anomalous resistivity is possible. The relative contributions of the various Galilean satellites for providing the ions in the plasma torus and sheet are assessed during the encounters.

The substantial periods of time that the Galileo spacecraft is located in the plasma sheet offer the unique opportunity to view the responses of the Jovian magnetosphere to the volcanic activity on Io. If specific Io volcanic eruptions can be identified with temporal fluctuations in densities, composition, and motions of the plasma sheet, remarkable advances in our knowledge of the transport of mass and momentum in the Jovian magnetosphere are envisioned.

Simultaneous observations of three-dimensional plasma velocity distributions and of plasma waves with the Galileo spacecraft allow the first studies of wave-particle interactions in the wide-ranging types of plasmas in the Jovian magnetosphere. A discussion of measurements of plasma waves during the Voyager encounters has been given by Gurnett and Scarf (1983). For example, the velocity distributions of ions can be examined to determine whether or not resonant acceleration by ion-cyclotron waves is an important mechanism for ion heating in the torus and plasma sheet. Further the amplitudes of broadband electrostatic noise can be compared with plasma velocity distributions to determine the importance of the anomalous resistivity in plasma heating. Free-energy sources, e.g., ring distributions in the electron velocity distributions, for the generation of electron cyclotron or upper hybrid waves may be identified and related to the wave amplitudes observed with the plasma wave instrument. In general the direct measurement of the plasma density and other parameters gives the growth, propagation and resonance conditions for plasma waves in wave-particle interactions. Thus the mechanisms for providing Jupiter with intense radio sources and particle precipitation into the auroral ionosphere can be further understood.

The existence of the magnetospheric wind at radial distances $> 130\ R_J$ in the dawn sector of the magnetosphere offers exciting goals for the orbit into the distant magnetotail. The origins of this wind are unknown. It is possible that the magnetospheric wind develops near the Alfvén point, where the corotational speed is equal to the Alfvén speed. The actual position must be determined from considerations of the tangential stress balance (cf. Vasyliunas, 1983). Thus magnetic bubbles could be slung radially outwards into the magnetotail. The low pressures in the magnetotail would produce super-Alfvénic radial outflow. On the other hand, the outflow wind might be thermally powered by the hot plasma in the plasma sheet inside the Alfvén point. A third possibility is that the magnetospheric wind is the signature of reconnection of magnetotail lines in a convection pattern controlled by dayside magnetic merging rates. The response of the magnetotail to fluctuating internal plasmas, e.g., Iogenic plasmas, or to a varying solar wind are unknown. In the magnetotail characterized by spectacular, explosive activity or a mere quiescent outflow of plasmas? The exploratory orbit into the magnetotail will indeed answer many questions concerning the origins and dynamics of this immense and little understood plasma region.

4. Overview of the Plasma Instrument

A pictorial view of the plasma instrument (PLS) is shown in Figure 1. The instrument is divided into two analyzers, A and B. Each electrostatic analyzer comprises three 70° spherical-segment plates. The outer and inner plates are grounded and the center plate is supplied with a programmed series of voltages to effect analyses of the energy spectra of electrons (E) and positive ions (P). The inner and outer channels between the plates are the positive ion and electron analyzers, respectively. A charged particle successfully passes through the channel on the basis of its energy-per-unit charge (E/Q). Continuous-channel electron multipliers, or Spiraltrons, are employed as sensors and are positioned

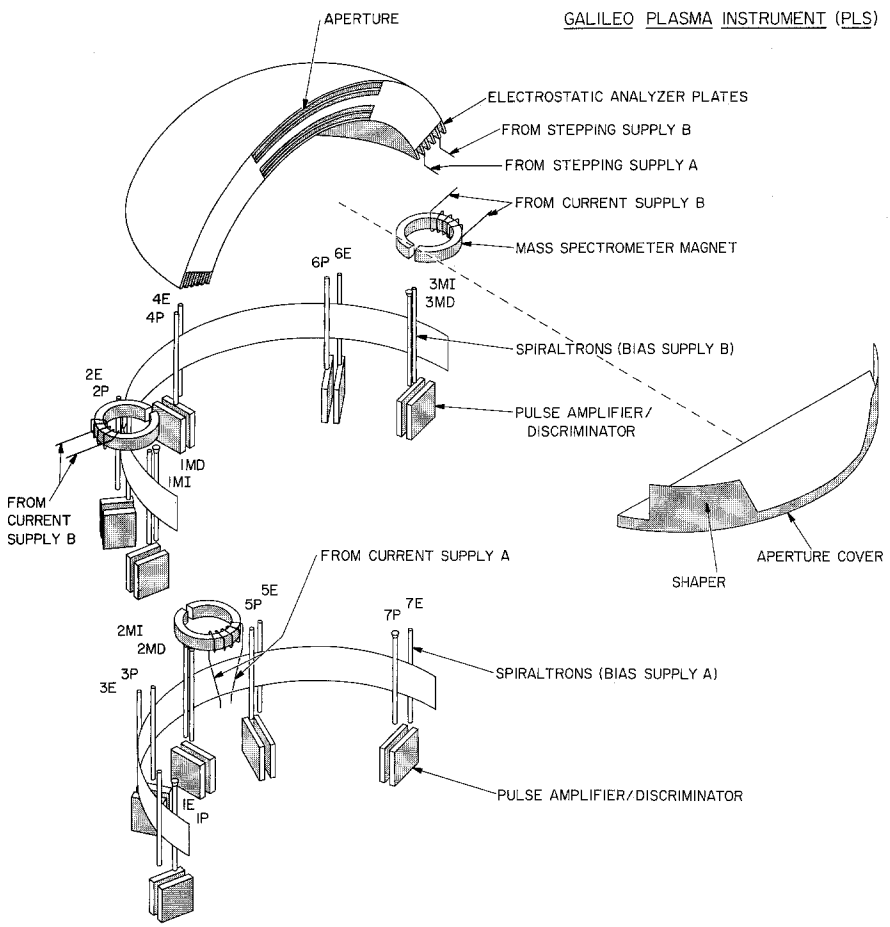

Fig. 1. An exploded view of the electrostatic analyzers, miniature mass spectrometers, and sensors of the plasma instrumentation (PLS) for the Galileo Mission.

at the exit apertures of the electrostatic analyzers. Charged particles arrive at positions at the exit aperture according to their direction of arrival at the entrance aperture. The analyzers are mounted on the instrument (magnetometer) boom of the spacecraft such that charged particles moving perpendicular to the spacecraft spin axis arrive at sensors $4E$ and $4P$, and particles generally moving parallel and anti-parallel to the spin axis are detected with sensor pairs $7E$, $7P$ and $1E$, $1P$, respectively. Thus the fan-shaped fields-of-view are divided into segments by the use of multiple sensors. The instantaneous fields-of-view for the seven ion sensors as projected onto the unit sphere for velocity vectors are shown in Figure 2. Rotation of the spacecraft spinning section allows coverage of almost the entire unit sphere and angular distributions are obtained by electronically sectoring the sensor responses as a function of spacecraft rotation angle. The angular sampling of electron velocity distributions is similar. The instrument

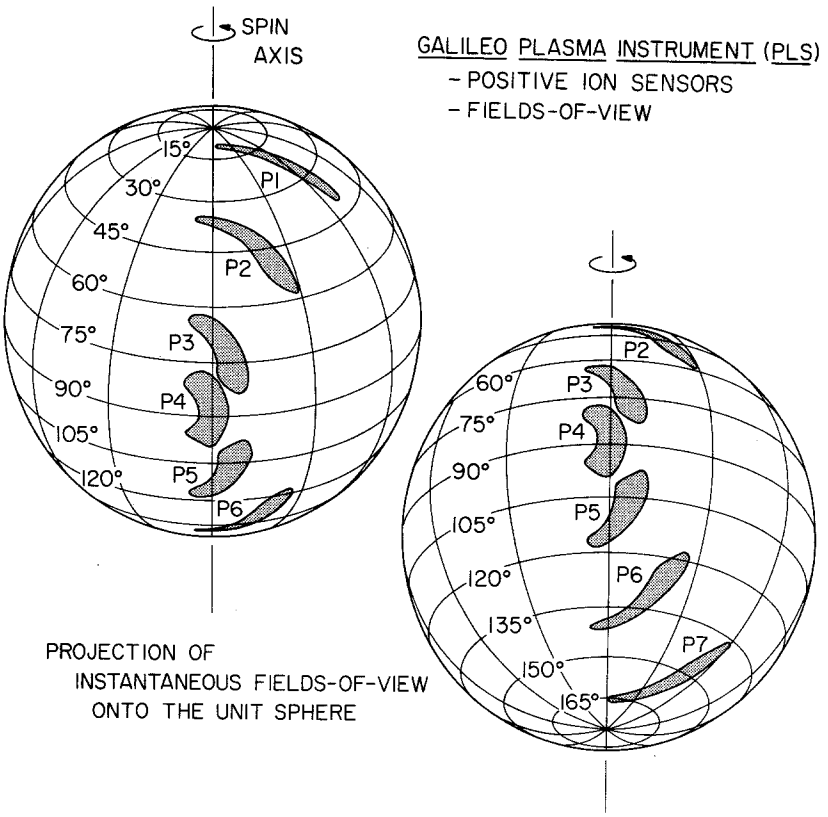

Fig. 2. The instantaneous fields-of-view for the seven positive ion sensors as projected onto the unit sphere. Rotation of the spacecraft spinning section provides coverage of 80% of the unit sphere for ion velocity vectors. The coverage of this solid angle with the seven electron sensors is similar.

is placed at a sufficient distance out along the boom to avoid obstruction of the fields-of-view by the large dish antenna of the spacecraft.

Three miniature mass spectrometers are included in the instrument for determining the composition, i.e., mass-per-unit charge (M/Q), of the positive ion plasmas. As shown in Figure 1 two of these mass spectrometers are positioned at the exit aperture of electrostatic analyzer B, the third spectrometer is in analyzer A. Each of these mass spectrometers is equipped with two Spiraltrons as sensors and an electromagnet. One of these sensors is placed behind the electromagnet such that it accepts ions not deflected by the gap magnetic field. These 'integral flux' sensors are shown as 1MI, 2MI, and 3MI. The second sensor in each mass spectrometer is displaced from the undeflected path and accepts ions with M/Q values that are a function of the gap magnetic field. These 'differential flux' sensors are 1MD, 2MD, and 3MD. A programmed series of currents is fed to the electromagnet. If the polar angle is taken as 0° in the direction of the spacecraft spin axis, then the fields-of-view are 11°–38°, 87°–93°, and 142°–169° for spectrometers 1, 2, and 3, respectively. The instantaneous fields-of-view

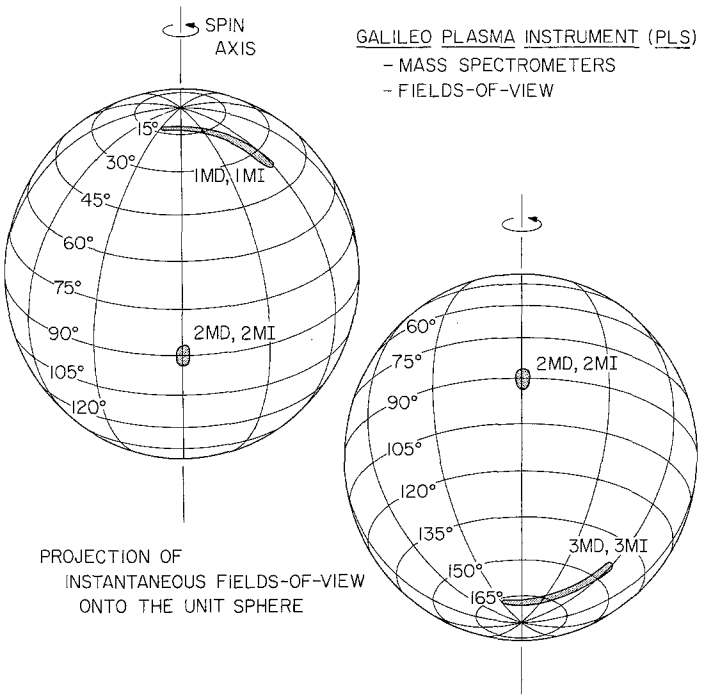

Fig. 3. The instantaneous fields-of-view for the three mass spectrometers as projected onto the unit sphere.

of the three mass spectrometers as mapped onto the unit sphere are shown in Figure 3.

The aperture cover shown in Figure 1 serves two purposes. Prior to and during launch the cover in its closed position prevents contamination of the sensors from dust and condensable vapors. After the launch sequence, the cover is opened and is employed to tailor the fields-of-view of the sensors viewing at small angles to the spin axis of the spacecraft. The corresponding obstructions are identified as shapers in Figure 1.

A photograph of the Galileo plasma instrument is shown in Figure 4, along with a 6-inch ruler. The aperture cover has been opened to show the two arc-shaped openings that are the entrance apertures for the two analyzers, A and B. A thermal blanket is yet to be installed around the instrument.

5. Design of the Instrumentation

5.1. Electrostatic Analyzer

The spherical-segment analyzer plates are precision-machined from solid blocks of magnesium. The radii of the inner and outer surfaces, respectively, of the four electrostatic analyzers are 9.68 and 9.95, 10.08 and 10.36, 11.77 and 12.10, and 12.23 and 12.57 cm. These plates are concentric. Thus the analyzer constant $C \simeq 18.2$, where

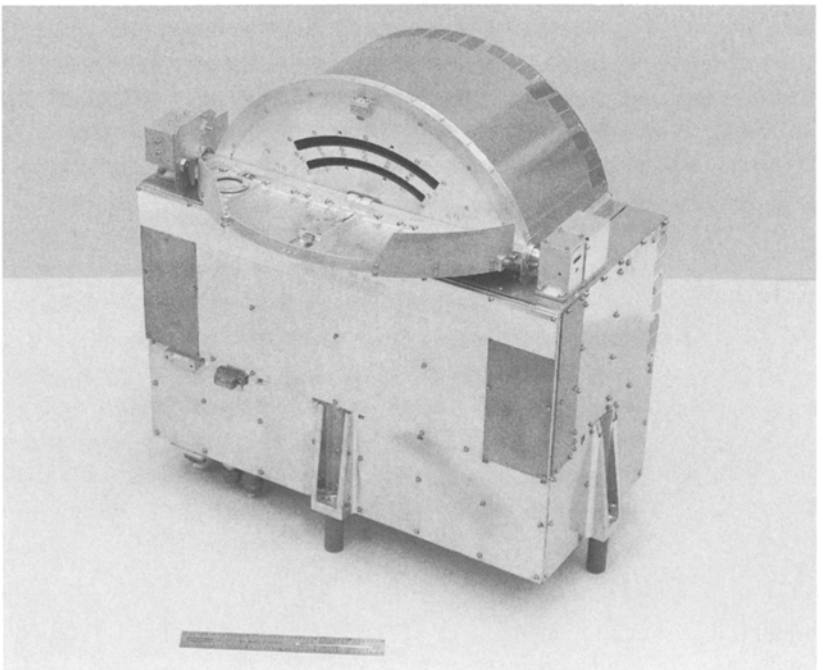

Fig. 4. Photograph of the plasma instrument. The two arc-shaped openings are the apertures for the two sets of electrostatic analyzers. A 6-inch ruler is shown for comparison.

$E/Q = CV$ and V is the plate voltage. The angle from the center of the entrance aperture to the exit aperture of the analyzer is 70° as referenced to the common center of curvature. Each of the concave surfaces within the analyzers has been machined with 140 saw-tooth serrations. The interior surfaces of the analyzer plates have been also electrodeposited with platinum black over gold electroplate. The two latter measures are taken in order to suppress the scattering of ultraviolet radiation and charged particles within the analyzers into the sensors. The entrance aperture is 60° wide. Because the entrance aperture is wide in order to provide good angular coverage in spacecraft latitude (see Figure 2), the fields-of-view shapers are used on the protective cover to limit excessive spreading in the azimuthal direction for the polar sensors. The center plate of each analyzer pair is supplied with voltages ranging from 0.05 to 2880 V in order to provide energy (E/Q) spectra of positive ion and electron intensities. The E/Q range is 0.9 eV q^{-1} to 53 keV q^{-1}. There are 64 plate voltages that cover this energy range in logarithmically equal increments. The averaged full-width at half maximum responses (FWHM) of the ion and electron passbands are equal, $\Delta E/E = 0.11$. The range and sequence of plate voltages can be selected by ground command.

A total of seven sensors are used for the two electron analyzers, and seven for the two positive ion analyzers. These continuous channel multipliers are Spiraltrons, model SEM 4211 with 1-mm diameter apertures and model SEM 4213 with 3-mm diameter apertures, manufactured by Galileo Electro-Optics Corporation. Entrance apertures of

these sensors are positioned at a distance 16 mm from the exit aperture of their respective electrostatic analyzers. The Spiraltrons with larger apertures are used for the two ion sensors that view closest to the spin axis of the spacecraft, i.e., the polar sensors, in order to offset the reduced projected area of the entrance aperture. The sensors are screened for stability by operation for $\sim 2 \times 10^9$ accumulated counts at a gain $\gtrsim 10^8$. Grounded mesh screens are mounted in front of the entrance apertures of the sensors to shield the sensor post-acceleration electric fields for the prevention of the collection of secondary charged particles produced in the interior of the instrument. The post-acceleration voltage for the ion sensors is approximately the bias voltage, and about + 150 V for the electron sensors. The nominal gain of the Spiraltrons is 5×10^7 to 3×10^8 in the saturated pulse counting mode. The output charge is collected by small plates and the collection efficiency is improved by a potential difference of about 120 V for the electron sensors and 200 V for the ion sensors. This charge is received by hybrid amplifiers and discriminators manufactured by AMPTEK Inc., model A101. The threshold for these amplifiers was conservatively set at 4×10^6 electrons. The high voltage for sensor bias is programmable by ground command in 32 increments spanning the range 2200 to 3800 V in order to maximize the operating lifetime of the sensors against degradation by using the minimum charge per pulse. The pulse pair resolution of the amplifier/discriminator is nominally 250 ns (4 mHz), and about 1.4 μs (700 kHz) after modification for use in the instrument.

5.2. Miniature mass spectrometers

Three miniature mass spectrometers are included in the plasma instrument, one spectrometer in analyzer *A* and two spectrometers in analyzer *B* as shown in Figure 1. A more detailed diagram of one of these small mass spectrometers is shown in Figure 5. After passage through the electrostatic analyzer the positive ions enter two collimating slits. The dimensions of the first slit are 11.1×0.15 mm and for the second slit, 8.5×0.15 mm. These two slits are separated by 9.5 mm. The paths of the positive ions are then deflected according to their M/Q by the magnetic field in the gap of a small electromagnet. The gap dimension is 3.0 mm and the length and width of the pole pieces are 9.9 and 4.0 mm, respectively. The magnet core is fabricated from a material similar to HY MU 80 and wound with about 5000 turns of $33\frac{1}{2}$-gauge silver wire. Overlapped sheets of Permalloy 80 with thickness 0.010 inch are used to encase the plasma instrument to reduce the maximum stray field to 16 nanotesla (nT) at a distance of 1 m. The mass of the electromagnet is 150 g. The electromagnet is supplied with a programmed series of 64 currents ranging from 0.6 to 105 mA. The sequence of current values can be controlled by ground command. The corresponding range of gap magnetic fields is 0.0014 to 0.225 T. The ions are detected with two Spiraltrons, one Spiraltron (integral) with a 1-mm aperture for undeflected ions, and one Spiraltron (differential) with a 3-mm aperture that is offset from the path for undeflected ions. The magnet is non-focussing and the 3-mm aperture Spiraltron is used to achieve approximately equal geometric factors for the differential and integral channels. The sensor apertures are positioned at a distance 20.1 mm from the exit face of the electromagnet. A slit with width 0.76 mm

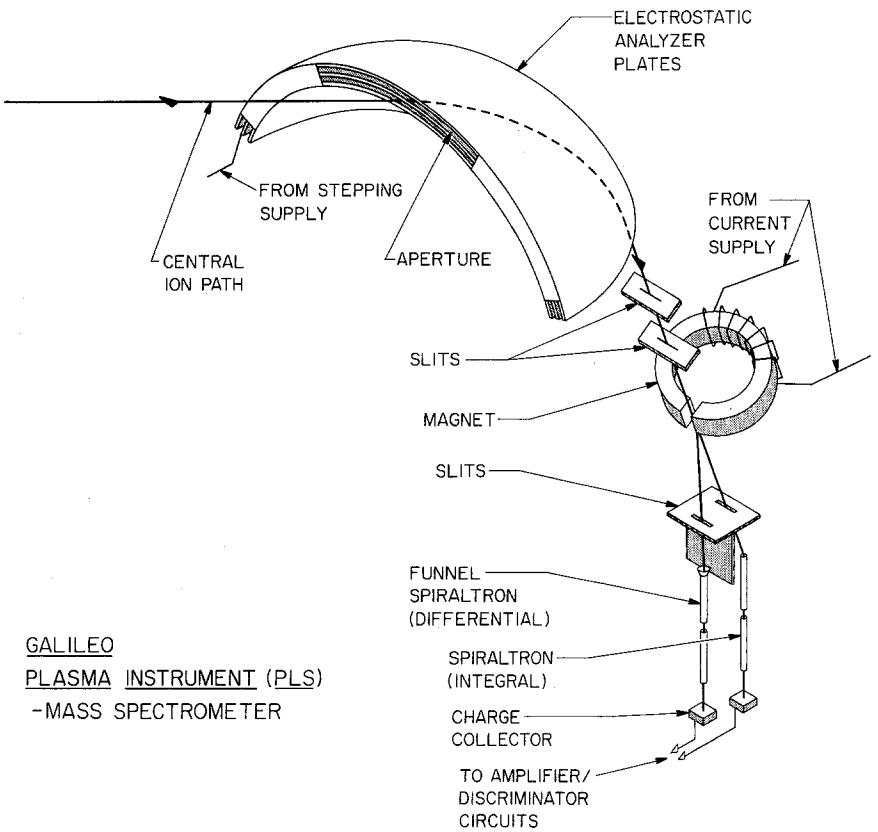

Fig. 5. Configuration of one of the three miniature, magnetic mass spectrometers in the plasma instrument.

is placed in front of each of the two Spiraltrons. The centers of these slits are separated by 3.30 mm. The Spiraltrons are operated in a similar manner as previously described for the sensors for the electrostatic analyzers.

An example of the mass spectrometer performance taken from laboratory calibrations of the flight instrument is shown in Figure 6. The value E/Q is 947 V for the two ions in the beam, H_2^+ and OH^+. The sweeping of the ions from the integral sensor as a function of M/Q and mass channel (magnet current) is clearly evident. At higher mass channels (larger current) these ions are deflected sufficiently to be detected with the differential sensor. A summary of the measured performance of the miniature mass spectrometer as functions of M/Q, E/Q, and electromagnet current is given in Figure 7. The M/Q value for the integral sensor is taken at a fraction 0.5 of the undeflected responses. For a given current step of the mass spectrometer, the averaged FWHM for the three mass spectrometers in terms of ion energy is $\Delta E/E = 0.06$. In general the differential channel is used for the detection of trace fluxes of light ions and the integral channel for abundant heavy ions in the Jovian magnetosphere. The mass resolutions

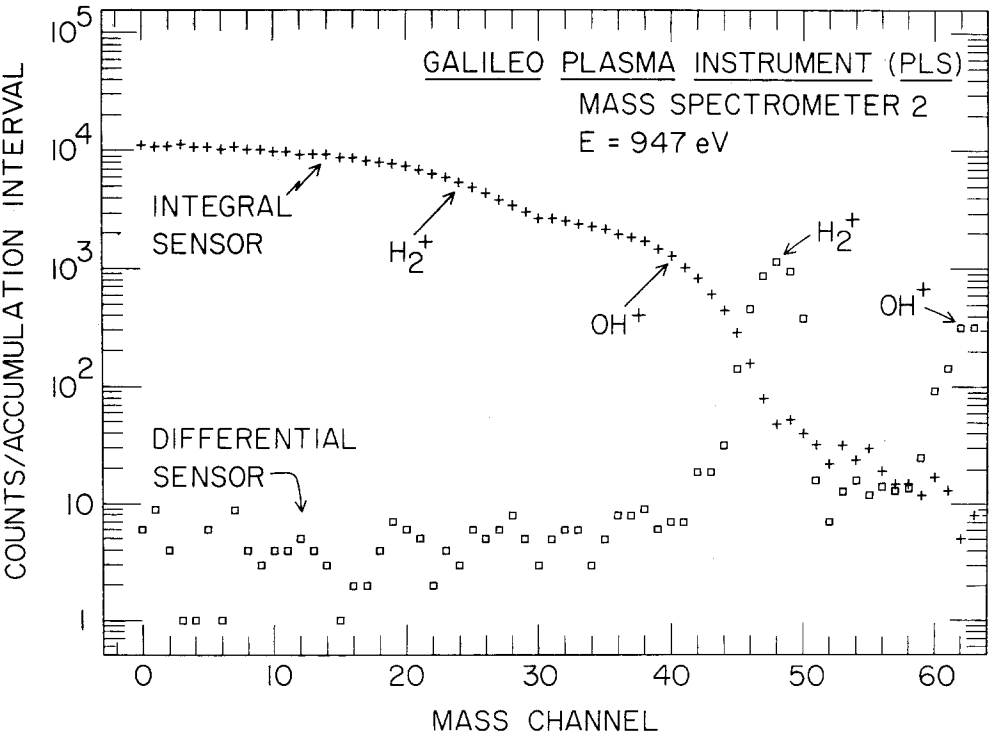

Fig. 6. Calibration of a miniature mass spectrometer with an ion beam (H_2^+, OH^+). The unresolved water group (O^+, OH^+, H_2O^+) is designated as OH^+. The beam energy is 947 eV and the beam current is constant. The responses of the integral and differential channels are shown as a function of electromagnet current (mass channel). The current increases by a logarithmically equal increment for each mass step.

of the mass spectrometers are $M/\Delta M = 4.1$ at full-width at 50% responses (FWHM) for the differential sensors (*MD*) and $M/\Delta M \simeq 2$ for the integral sensors (*MI*). This resolution has been chosen to allow identification of the species H^+, H_2^+ (He^{++}), He^+, O^{++}, O^+, Na^+, S^+, and K^+ with the *MD* sensors and H^+, H_2^+ (He^{++}), O^{++}, O^+, S^+, and SO_2^+ with the *MI* sensors. The E/Q ranges vary with the M/Q of the ion species, e.g., for the *MD* sensors, 0.9 V to 20 keV for H^+, 0.9 V to 3 kV for O^+, and 0.9 V to 800 V for S^+. For the *MI* sensors, these ranges are 10 V to 52 kV for H^+, 0.9 V to 52 kV for O^+, and 0.9 V to 14 kV for S^+. The mass spectrometers cannot distinguish between two ions with the same M/Q, e.g., O^+ and S^{++}. The mass spectrometers are designed in part with the criterion that corotating SO_2^+ ($M/Q = 64$ amu, $E/Q \simeq 2$ kV) can be identified at Io's orbit.

5.3. Geometric factors

A summary of the latitudinal coverage, energy resolutions, and geometric factors of each of the twenty sensors in the plasma instrument is given in Table I. The averaged geometric factors for the electron and positive ion sensors of the electrostatic analyzers

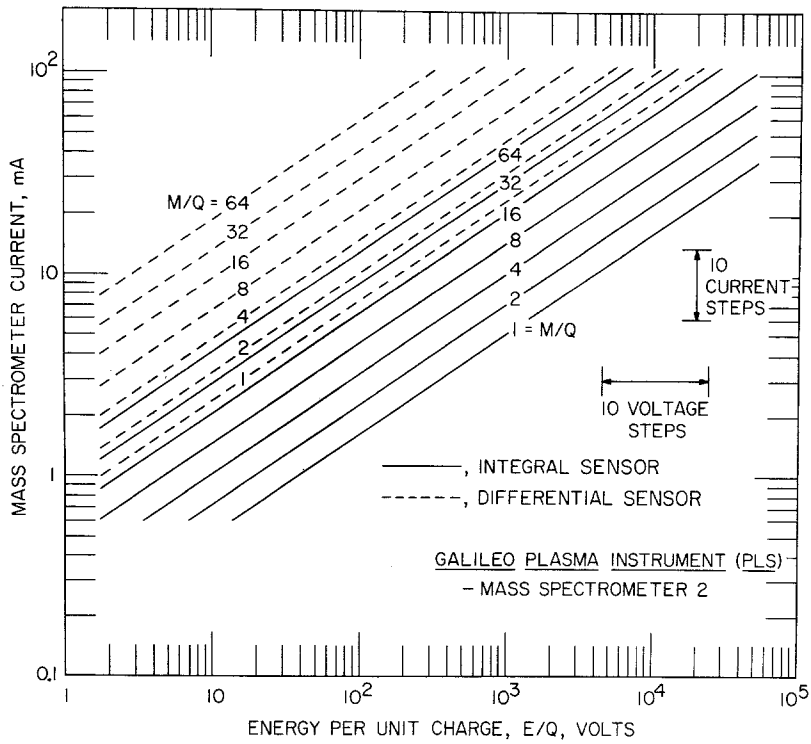

Fig. 7. The relationship of energy-per-unit charge (E/Q), mass spectrometer current, and mass-per-unit charge (M/Q) for the detection of positive ions with the miniature mass spectrometers. The E/Q value is 960 V for a corotating S^+ ion at equatorial radial distance 6 R_J in the Jovian magnetosphere.

and the positive ion sensors of the mass spectrometers are 3.4×10^{-5}, 6.4×10^{-5}, and 3.2×10^{-6} cm^2 sr eV eV^{-1}, respectively.

These values are computed by comprehensive ray tracing of trajectories through the electrostatic and magnetic analyzers and with the nominal entrance area of the sensor. In practice both the efficiency and this area vary with individual sensors and final values of the geometric factors are derived from laboratory measurements and inflight responses in an isotropic plasma such as that in the plasma sheet during Earth1 encounter. These geometric factors are tailored to provide effective measurements of both the dense plasmas in the torus and the sparse plasmas of the outer Jovian magnetosphere.

The sensitivities for detecting these plasmas are summarized in Figure 8. The maximum responses of a single sensor to several representative plasmas are shown as functions of the plasma temperature, bulk flow speed V, and species. The bulk speed of 100 km s^{-1} has been chosen as scale-wise representative for the corotational speeds in the torus. The densities of all the plasmas are each assumed to be 1 cm^{-3}. For example, if the density of S^+ ions is 1000 cm^{-3}, V is 100 km s^{-1}, and the temperature kT is 100 eV, the maximum responses of the ion sensors of the electrostatic analyzer

TABLE I

Galileo PLS performance parameters

Sensor	Polar angle coverage, θ	Energy resolution, $\Delta E/E$ at FWHM	Geometric factor[b], cm^2 sr eV eV^{-1}
Electrons			
Energy range: 0.9 V $\leq E/Q \leq$ 52 kV			
1*E*	14°–41°	0.14	1.9×10^{-5}
2*E*	38°–62°	0.12	3.7×10^{-5}
3*E*	58°–80°	0.10	4.1×10^{-5}
4*E*	81°–102°	0.08	5.0×10^{-5}
5*E*	100°–122°	0.10	4.1×10^{-5}
6*E*	121°–146°	0.12	3.6×10^{-5}
7*E*	142°–171°	0.14	1.3×10^{-5}
Positive ions			
Energy range: 0.9 V $\leq E/Q \leq$ 52 kV			
1*P*[a]	9°–41°	0.15	9.8×10^{-5}
2*P*	35°–59°	0.12	3.5×10^{-5}
3*P*	62°–84°	0.09	4.1×10^{-5}
4*P*	78°–99°	0.07	5.0×10^{-5}
5*P*	97°–119°	0.09	4.0×10^{-5}
6*P*	118°–141°	0.11	3.6×10^{-5}
7*P*[a]	136°–166°	0.15	1.5×10^{-5}
Ion composition			
Energy range: species dependent			
Differential (*D*) sensor:	0.9 V to 20 kV (H^+)		
	0.9 V to 800 V (S^+)		
Resolves:	H^+, H_2^+, He^+, O^+, Na^+, S^+, K^+ with $M/\Delta M = 4.1$		
Integral (*I*) sensor:	10 V to 52 kV (H^+)		
	0.9 V to 14 kV (S^+)		
Resolves:	H^+, H_2^+, He^+, O^+, S^+, SO_2^+ with $M/\Delta M \simeq 2.0$		
1*MD*[a], 1*MI*	11°–38°	0.03	2.4×10^{-6}
2*MD*[a], 2*MI*	87°–93°	0.03	4.7×10^{-6}
3*MD*[a], 3*MI*	142°–169°	0.03	2.4×10^{-6}

[a] 3-mm entrance diameter, others are 1 mm.

[b] Preliminary values based upon ray tracing (see text).

(*P*) and of the ion sensors of the mass spectrometers (*M*) are 4×10^6 and 2×10^5 counts s^{-1}, respectively, when viewing in the bulk flow direction. The geometric factor of the ion sensor (*P*) is sized such that these responses are somewhat above the saturation values for the sensor/amplifier, $\sim 10^6$ counts s^{-1}. The ion sensors in the mass spectrometers are employed to extend the dynamic range of these ion measurements to the larger ion densities by means of their lesser geometric factors. On the other hand, the large geometric factor of the ion sensors for the electrostatic analyzers provides the capability of the determining densities of hot ($\sim$ tens of keV), isotropic ions as low as 10^{-3} to 10^{-2} cm^{-3} in the outer regions of the magnetosphere. Thus the

combined geometric factors of the electrostatic analyzers and mass spectrometers accommodate a large range of ion densities. If the electron densities in the center of the plasma torus are 3000 cm^{-3}, then the maximum responses for the electron sensors are $\sim 2 \times 10^5$ and 6×10^5 counts s^{-1} for electron temperatures $kT = 1$ and 10 eV, respectively. For an electron temperature of 10 keV in the outer magnetosphere, densities as low as 10^{-4} to 10^{-3} cm^{-3} can be well determined.

Considerable attention in the design of the instrument was directed toward minimizing the sensor responses to the intense fluxes of energetic electrons in the inner Jovian magnetosphere. The Spiraltrons are shielded in all directions by a minimum of 2.5 g cm^{-2} equivalent of aluminum. This corresponds to an electron range of ~ 5 MeV. In addition the Spiraltrons used for ion sensors are operated at a sufficiently low voltage that two or more initial secondary electrons at their entrance apertures are necessary to yield an electron pulse above the discriminator level of the amplifiers. This mode of operation reduces the sensor efficiency for the detection of ions by 50% ($\pm 10\%$), with a corresponding decrease in the geometric factors cited in Table I. Such operation of the sensors at bias voltages ~ 2400 V allows discrimination against detection of penetrating electrons. The omnidirectional geometric factors for detection of penetrating, $\gtrsim 5$ MeV electrons are $\sim 10^{-4}$ cm^2 for the ion sensors with 1-mm apertures, and $\sim 10^{-3}$ cm^2 for the 3-mm ion sensors (see Table I). The corresponding geometric factors for the Spiraltrons used in the electron analyzers are $\sim 10^{-3}$ cm^2. At the orbit of Io the electron intensities with $E \gtrsim 5$ MeV are $\sim 2 \times 10^7$ cm^{-2} s^{-1} (Van Allen, 1976). Thus the background counting rates are $\sim 2 \times 10^3$, 2×10^4, and 2×10^4 counts s^{-1} for the 1-mm ion sensors, the 3-mm ion sensors, and the 1-mm electron sensors, respectively. For comparison, the sensor responses in the direction of flow (S^+, 1000 cm^{-3}, 50 eV, 100 km s^{-1} from Figure 8) are $\sim 5 \times 10^6$ counts s^{-1} for the ion channels of the electrostatic analyzer and $\sim 3 \times 10^5$ counts s^{-1} for the sensors in the mass spectrometer. The analyzer responses to electrons (e^-, 1000 cm^{-3}, 50 eV from Figure 8) are expected to be $\sim 6 \times 10^5$ counts s^{-1}. The corresponding S/N ratios are 2500, 150 (I), and 15 (D), and 30 for the ion sensors, mass spectrometer sensors, and electron sensors, respectively.

At larger radial distances, $\gtrsim 20\ R_J$, the intensities of electrons with $E \gtrsim 5$ MeV are typically $\lesssim 10^3$–10^4 cm^{-2} s^{-1} within and near the plasma sheet (Baker and Van Allen, 1976). The corresponding maximum background rates are then $\lesssim 1$ and 10 counts s^{-1} for the 1-mm positive ion and electron sensors, respectively. For these maximum rates, the densities for which $S/N = 1$ for an isotropic, H^+ plasma are 3×10^{-3} cm^{-3} at $kT = 10$ keV and 5×10^{-3} cm^{-3} for electrons at 1 keV (see Figure 8). The corresponding densities for the mass spectrometer sensors are ~ 0.1 cm^{-3} (I) and 1 cm^{-3} (D). These above examples for H^+ give the most pessimistic values because we have assumed worst-case background rates and because the ion plasmas are partially corotating. The S/N ratios will be typically larger by factors of ~ 10 to 100.

The spacecraft potential is expected to be important at the lower energy range of the analyzer. A quantitative assessment of anticipated spacecraft potentials is given by the Voyager plasma measurements. In the outer magnetosphere, typical Voyager spacecraft

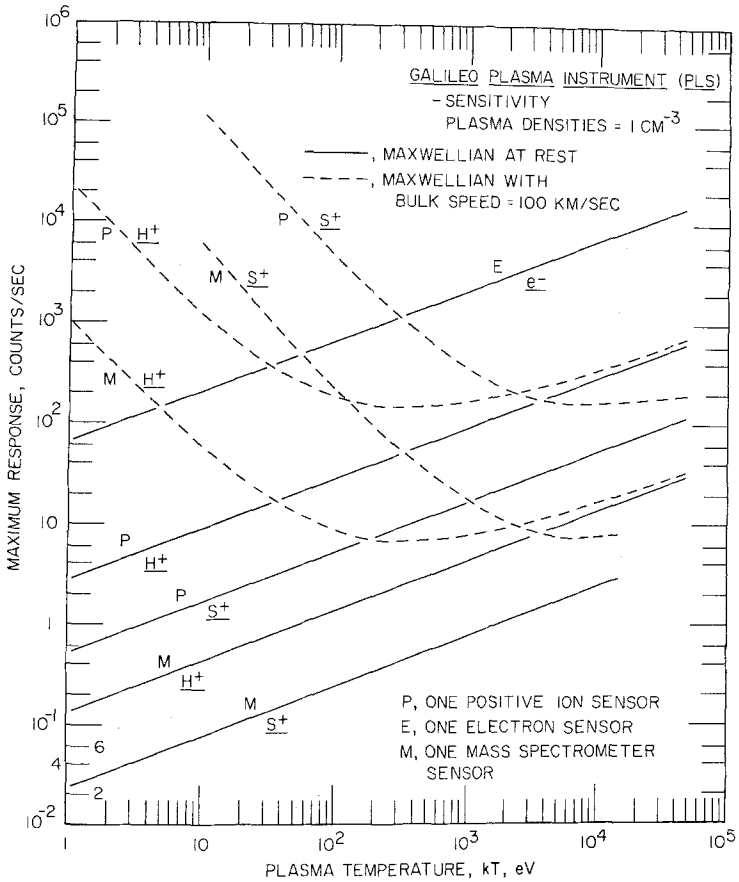

Fig. 8. Maximum responses of several individual sensors to a Maxwellian plasma distribution as a function of plasma temperature. Responses to H^+ and S^+ plasmas at rest and with bulk flow speed 100 km s^{-1} are shown. The densities of electron and ion plasmas are each taken as 1 cm^{-3}.

potentials were positive in the range of several volts to 10 V (Scudder *et al.*, 1981). Because the plasmas are generally hot, temperatures ~ keV, in the outer magnetosphere the plasma measurements should not be greatly impaired. On the other hand, in the highest density regions of the Io torus, Voyager spacecraft potentials were negative with magnitudes up to 25 V (Sittler and Strobel, 1987). In this region electron temperatures are tens of eV or less and the observations of thermal electron plasmas may be precluded if the Galileo spacecraft potential is similar. The energy range of the Galileo plasma instrument is sufficient to determine this spacecraft potential. Determination of the magnitude of the potential will have to await the *in-situ* observations. The potentials along the boom on which the plasma instrument is mounted and those of the spacecraft body will also affect the trajectories of low-energy particles as viewed by the plasma analyzer. This effect will have to be modeled in detail in order to determine the deflections of the observed angular distributions as a function of the particle energy.

5.4. INSTRUMENT ELECTRONICS

The plasma instrument is divided into two analyzer systems *A* and *B* as shown in Figure 9 (see also Figure 1). This configuration of the instrument has been chosen in

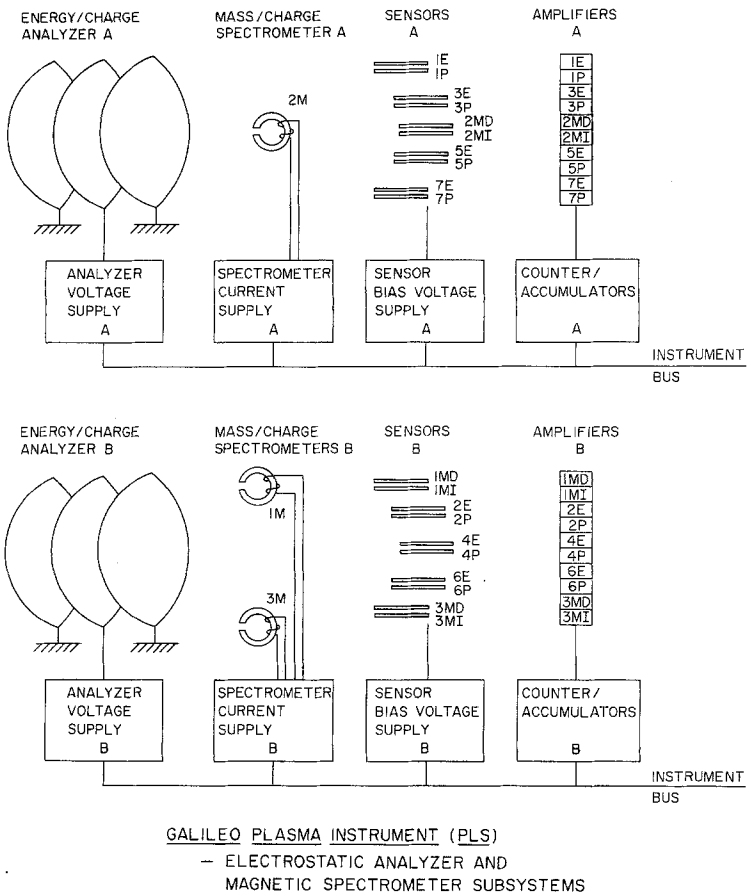

Fig. 9. Block diagram for the two analyzers, *A* and *B*, in the plasma instrument.

order to reduce the number of possible single-point failures that could result in the total loss of the scientific objectives. Each analyzer is equipped with a set of electrostatic analyzer plates, at least one miniature mass spectrometer, and a partial set of the sensors for the measurements of the three-dimensional velocity distributions of positive ions and electrons. A dedicated plate voltage supply, magnet current supply, and sensor bias voltage supply are provided for each analyzer. Each sensor is serviced by a 16-bit accumulator. The electronics for both analyzers are controlled from the instrument bus.

The reduction of single-point failures of the instrument proved to be considerably more difficult for the data handling and control subsystem (DHCS). The configuration

that was chosen for the microprocessors and associated electronics is shown in Figure 10. There are two separate buses, *A* and *B*, that can singly operate the two analyzers shown in Figure 9. Similarly there are two RCA 1802 microprocessors, 1 and 2, that are each equipped with 4 kbytes of read-only memory (ROM) and 4 kbytes of

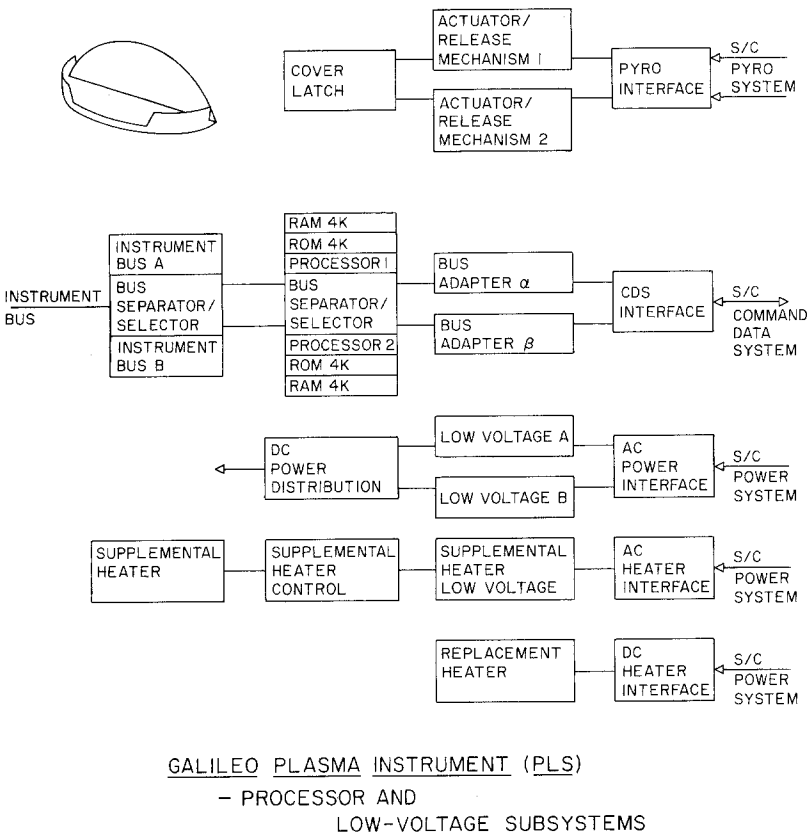

Fig. 10. Block diagram for the electronics in the plasma instrument. Two microprocessors are used to improve the reliability.

read/write memory (RAM). Two bus adapters, α and β, couple the microprocessors with the command data system (CDS) of the spacecraft. The instrument is operated with one bus adapter, one microprocessor, and one bus. The bus separator/selector allows the use of any combination of these electronic elements, e.g., bus adapter α, processor 2, and instrument bus *A*. This configuration for the DHCS is set via a hardware bus command (HBC) that transfers the necessary information in the address portion of the packet header from the spacecraft CDS. The HBC is executed regardless of which processor and bus adapter are currently selected. If the currently selected bus adapter fails, the HBC can be used to select the other bus adapter.

Each of the two microprocessors is provided with identical I/O electronics that include an analog-to-digital (ADC) converter (model AD571, Analog Devices, Inc.), three digital-to-analog (DAC) converters, and a digital status input port. A 16-input multiplexor is used with the ADC to monitor voltages within the instrument. The DACs provide the control voltages for the programmable high voltage (plate and bias) and current (electromagnet) supplies.

Two low-voltage power supplies, *A* and *B*, are included within the plasma instrument. By means of a power distribution system, failure of a single low voltage supply does not result in the loss of the DHCS or instrument bus. Analyzer *A* or *B* becomes inoperable with the failure of the one of the low-voltage power supplies, *A* or *B*. A power switching circuit that is controlled by ground command is used to select the analyzer to be operated with the functioning low-voltage power supply. The replacement and supplemental heaters shown in Figure 10 are used for thermal control during the mission. The latch for releasing the protective cover over the instrument aperture is a one-shot redundant device with two electrically fired, black powder Unidynamics bellows actuators.

5.5. Mass, size, and power

The overall dimensions of the plasma instrument are 8.00 × 15.00 inch (mounting surface) and 13.68 inch (height). The total mass is 13.2 kg, of which 0.33 kg is used for magnetic shielding and 3.57 kg is invested in radiation shielding of the sensors and electronics with tantalum. The average power, without heaters, is dependent upon the electronic configuration of the instrument and is in the range of 6.5 to 10.7 W.

6. Inflight Operation of the Instrument

The operating modes of the plasma instrument are designed to accommodate the diverse plasmas in the Jovian magnetosphere. We provide here a brief introduction to those capabilities. The instrument cycle time is 243 s and is subdivided into 12 equal intervals, or instrument spin modes. Each spin mode is a separate instrument operations and data collection cycle. The duration of a spin mode is 20.3 s and thus slightly longer than the range of anticipated rotation periods for the spacecraft spinning section, 18.3 to 19.8 s. By ground command the plasma instrument can be configured to sample a combination of a given set of sensors, a range of energy passbands, a range of mass channels, and a set of angular sectors as the fields-of-view rotate. The operations of analyzers *A* and *B* can be programmed independently. Limitations of these analyzers are imposed by the minimum dwell time for the energy passbands and mass channels of 8.3 ms, a service time of 1 ms for the processing of the contents of a count accumulator, and the telemetry rate allocated to the instrument of 612 bits s^{-1} (72 sensor samples s^{-1} plus overhead). Each sample of sensor responses is quasi-logarithmically compressed into an 8-bit word. Internal buffers can allow rapid bursts of $\lesssim 1500$ measurements to be trickled into the telemetry stream.

Consider the measurement cycle time of the plasma instrument if onboard software were not available to improve the operational efficiency. If all energy passbands, mass

channels, and sensors were sampled in each of 16 angular sectors, then the time for this complete plasma measurement (1.3×10^6 samples) would be 5.1 hours. Such instrument operation is ineffective and wasteful of the capabilities for obtaining plasma parameters, e.g., individual 64-point energy or mass spectra in 0.5 s. Thus the spin modes are each designed to obtain a specific type of plasma measurement during one spacecraft rotation, e.g., a three-dimensional velocity distribution, high angular and energy resolutions of an ion beam, and the mass composition of an ion beam. A spin mode is constructed of nested control loops. These loops control (1) the number of angular sectors sampled during a spacecraft rotation, (2) the number of energy passbands or mass channels in a sector, (3) the duration of an energy passband or mass channel, (4) the readout of the selected sensors, (5) the sequence of energy passbands, and (6) the sequence of mass channels. Four sequencing tables are used to determine the operation of the instrument during a spin mode: (1) sensor, (2) mass channel, (3) energy passband, and (4) angular sector. The angular sectors are referenced to a fixed position on the celestial sphere by means of information from the spacecraft attitude control system. Instrument software is available for five basic types of spin modes. Default values for the sequence tables are also included in read-only memory in the instrument processor in lieu of values from ground commands. We briefly illustrate below the capabilities of the various spin modes.

Spin mode 1. Survey of positive ion and electron velocity distributions. All electron, ion, and integral ion sensors (spectrometers) are sampled. The number of angular sectors, the energy range, and the number of energy passbands are selected by ground command. The product of the numbers of passbands and angular sectors is 64. For example, the responses of all of the above sensors for 64 passbands sampled in a single angular sector of 45° can be telemtered each spacecraft spin period. Alternately 16 passbands (every fourth passband) in each of our 90°-sectors can be telemetered during a single rotation period in order to obtain the principal features of the three-dimensional velocity distributions of positive ions and electrons once each 20.3 s.

Spin mode 2. Determination of the velocity distribution of a positive ion beam. Electron and ion sensors corresponding to those nearest the direction of the ion beam are selected. These sensors and the spacecraft rotation angle for the beam are determined with measurements from a preceding spin mode 1. The rapid energy scans in the direction of the beam are limited to the energy range of the beam as determined during spin mode 1. For example, during one spacecraft rotation, energy passbands 8 through 23 can be sampled with three sensors for positive ions and two or three sensors for electrons for each of five contiguous 22.5°-sectors in the direction of the beam. Two electron sensors are used for analyzers *A* and *B*, with the exception of three for analyzer *B* if the beam is nearly perpendicular to the spacecraft spin axis. Again angular size of the sectors and the number of energy passbands can be selected by ground command.

Spin mode 3. Survey of ion composition. Mass spectrometers 1 and 2 are sampled for a selected range of gap magnetic fields. During one spacecraft rotation a single energy passband of the electrostatic analyzer is used and the gap magnetic fields are incremented over a selected series of values. Thus for a given energy passband and a single

spacecraft rotation it is possible to sample the entire M/Q range in 64 current steps in each of four 90°-sectors.

Spin mode 4. Survey of ion composition. This spin mode is identical to spin mode 3 with the exception that mass spectrometer 3 replaces 1.

Spin mode 5. Determination of the composition of an ion beam. The mass spectrometer with direction of field-of-view nearest to that of the ion beam is chosen on the basis of previous measurements with spin mode 1. The energy passband and angular sectors for the ion beam are similarly identified. For example, during one spacecraft rotation in the plasma sheet or torus of the Jovian magnetosphere full coverage of the M/Q range in 64 channels can be sampled in each of five contiguous 22.5° sectors.

The instrument cycles for analyzers A and B are each selected as a sequence of 12 spin modes. The order of the spin modes and their operating parameters such as energy and mass ranges, angular resolution, etc., are controlled by the sequence tables. As an example, a sequence of spin modes during an instrument cycle for analyzer A can be 1, 1, 2, 1, 1, 5, 1, 1, 4, 1, 1, 3. Thus the various operating modes of the plasma instrument can be implemented and cycled automatically with minimal demand for command uplinks to the Galileo spacecraft. Major command sequences are used to restructure the spin modes and their sequencing for special events such as the close encounters with the Galilean satellites and the exploratory survey into the distant magnetotail.

Acknowledgements

At The University of Iowa L. A. Frank is principal investigator and K. L. Ackerson is a co-investigator for the plasma investigation. The other co-investigators are F. V. Coroniti of the University of California at Los Angeles and V. M. Vasyliunas of the Max-Planck-Institüt für Aeronomie, Lindau, Germany. E. C. Stone of the California Institute of Technology is a co-investigator whose responsibility is the Heavy Ion Composition (HIC) investigation which employs a separate instrument on the Galileo Orbiter. The authors wish to express their appreciation to the following personnel of the Jet Propulsion Laboratory for their assistance in the implementation of the plasma instrumentation: J. R. Casani, W. G. Fawcett, H. W. Eyerly, C. M. Yeates, M. S. Spehalski, W. J. O'Neil, R. F. Ebbett, and T. V. Johnson. This research was supported in part at The University of Iowa by the Jet Propulsion Laboratory under contract 958778.

References

Bagenal, F.: 1985, 'Plasma Conditions Inside Io's Orbit: Voyager Measurements', *J. Geophys. Res.* **90**, 311.

Bagenal, F., McNutt, R. L., Jr., Belcher, J. W., Bridge, H. S., and Sullivan, J. D.: 1985, 'Revised Ion Temperatures for Voyager Plasma Measurements in the Io Plasma Torus', *J. Geophys. Res.* **90**, 1755.

Baker, D. N. and Van Allen, J. A.: 1976, 'Energetic Electrons in the Jovian Magnetosphere', *J. Geophys. Res.* **81**, 617.

Belcher, J. W.: 1983, in A. J. Dessler (ed.), 'The Low-Energy Plasma in the Jovian Magnetosphere', *Physics of the Jovian Magnetosphere,* Cambridge University Press, Cambridge, p. 68.

Frank, L. A., Ackerson, K. L., Wolfe, J. H., and Mihalov, J. D.: 1976, 'Observations of Plasmas in the Jovian Magnetosphere', *J. Geophys. Res.* **81**, 457.

Gurnett, D. A. and Scarf, F. L.: 1983, in A. J. Dessler (ed.), 'Plasma Waves in the Jovian Magnetosphere', *Physics of the Jovian Magnetosphere,* Cambridge University Press, Cambridge, p. 285.

Krimigis, S. M. and Roelof, E. C.: 1983, in A. J. Dessler (ed.), 'Low-Energy Particle Population', *Physics of the Jovian Magnetosphere,* Cambridge University Press, Cambridge., p. 106.

Sands, M. R. and McNutt, R. L., Jr.: 1988, 'Plasma Bulk Flow in Jupiter's Dayside Middle Magnetosphere', *J. Geophys. Res.* **93**, 8502.

Scudder, J. D., Sittler, E. C., Jr., and Bridge, H. S.: 1981, 'A Survey of the Plasma Electron Environment of Jupiter: A View from Voyager', *J. Geophys. Res.* **86**, 8517.

Sittler, E. C. and Strobel, D. F.: 1987, 'Io Plasma Torus Electrons: Voyager 1', *J. Geophys. Res.* **92**, 5741.

Van Allen, J. A.: 1976, in T. Gehrels (ed.), 'High-Energy Particles in the Jovian Magnetosphere', *Jupiter,* University of Arizona Press, Tucson, p. 928.

Vasyliunas, V. M.: 1983, in A. J. Dessler (ed.), 'Plasma Distribution and Flow', *Physics of the Jovian Magnetosphere*, Cambridge University Press, Cambridge, p. 395.